Pergamon

Cement and Concrete Research 33 (2003) 271–279

CEMENT AND CONCRETE RESEARCH

Thermal treatment of C–S–H gel at 1 bar H_2O pressure up to 200 °C

F.P. Glasser *, S.-Y. Hong

Department of Chemistry, University of Aberdeen, 033 Meston Building, Old Aberdeen, AB24 3UE Aberdeen, Scotland, UK

Received 28 February 2002; accepted 23 July 2002

Abstract

Homogeneous $CaO–SiO_2–H_2O$ gels were prepared at Ca/Si molar ratios 0.83, 1.01, 1.21, 1.50, 1.83 and 2.02. These were aged for 12–24 months at 25 °C and subsequently treated in steam, 1 bar total pressure, at 130 or 200 °C; also in water at 55 and 85 °C. Gels with low Ca/Si ratios partially crystallised at 85 °C. At 130 °C in steam, crystalline products included 11 and 14 Å tobermorite, xonotlite, afwillite, portlandite and another incompletely characterised phase. At 200 °C, the gels retained much water but remained amorphous to X-ray powder diffraction (XRD). However, electron microscopy, coupled with diffraction and analysis, disclosed that the ''amorphous'' product obtained at 85–200 °C had undergone crystallisation with domains typically 10–1000 nm. At higher bulk Ca/Si ratios, 1.83 and 2.02, much nanoscale precipitation of $Ca(OH)_2$ occurs, probably by exsolution, such that the residual C–S–H product has a Ca/Si ratio in the range 1.4–1.5. The complex thermal history of the products is reflected in their pH conditioning ability, measured at 25 °C. The results are applied to predict the evolution of pH in a cement-conditioned nuclear waste repository which experiences a prolonged thermal excursion.

Keywords: C–S–H gel; $CaO–SiO_2–H_2O$ system; $CaO–SiO_2–H_2O$ phases 20–200 °C; Steam treatment of C–S–H; Hydrothermal treatment

1. Introduction

In normal civil engineering practise, Portland cement constructions do not experience service temperatures exceeding 60–70 °C, although exceptions do occur. For example, the autoclaved cement industry is well developed: cements also encounter high service temperatures, >100 °C, in geothermal applications and in oil and gas wells. Experience suggests that the high Ca/Si ratio, ~3, of ordinary Portland cements leads to loss of strength at elevated temperatures. Silica is usually added in reactive form, e.g., as quartz flour, fly ash, etc., to lower the bulk Ca/Si ratio to 0.8–1.5. This leads to development of phases such as tobermorite, xonotlite and possibly afwillite, which enable better strength retention and reduced solubility in an aqueous phase, relative to either OPC or $Ca(OH)_2$ or mixtures [1].

Another type of high-temperature pulse, often of prolonged duration (10–1000 years), may occur in underground nuclear waste repositories. The thermal pulse is generated in the post-closure phase and its magnitude and duration depend on, among other factors, waste type, amount of waste and its density or distribution in the drift or vault.

Cement and concrete may be introduced into repositories for many purposes. For example, where retrievability is a requirement excavated cavities may be stabilised by engineering concrete liners. Cement and cement-related materials are also used in some repository designs to condition waste by reducing radionuclide solubility as well as forming a physical barrier to retard release of radionuclides.

In one projected scenario for the proposed repository at Yucca Mountain, USA, drifts are lined with concrete to protect their integrity during the constructional and operational as well as maintain retrievability, should it be required. The drifts will be vented during the operational phase with the result that temperatures will remain close to ambient. But in the post-closure phase, depending on waste loadings, temperatures could reach a maximum of 160–200 °C in the vaults. The country rock, a volcanic tuff, contains pore water. This pore water may be liberated locally as steam during the thermal pulse. However, as the thermal pulse decays, steam may condense and permeate the concrete liner where it will subsequently contact other man-made barriers, e.g., corrosion-resistant alloys protecting the waste matrix. While the corrosion behaviour of these alloys

* Corresponding author. Tel.: +44-272-171-906; fax: +44-1224-272-908.

E-mail address: f.p.glasser@abdn.ac.uk (F.P. Glasser).

0008-8846/02/$ – see front matter © 2002 Elsevier Science Ltd. All rights reserved.
PII: S0008-8846(02)00959-6

is well researched at the near-neutral pH of Yucca mountain groundwater and of simulate rock pore water, concern has been expressed that contact with concrete liners could alter the chemistry of percolating water, in which case the consequences to corrosion behaviour of alloy barriers become less certain. Moreover, it is unsatisfactory to argue the extent to which chemical alteration of percolating water will occur from the properties of fresh Portland cement paste, since significant percolation will only occur after the thermal pulse decays, by which time the hydrate composition may have been altered. A search of the literature revealed that the available data on the nature, extent and consequences of thermal alteration to cement are insufficient to predict a scenario with confidence.

While many studies of the $CaO–SiO_2–H_2O$ system have been made, these were typically done at saturated steam pressure, whereas in a vented repository pressure would remain fixed at 1 bar. Particularly at temperatures above 100 °C, data obtained in saturated steam, i.e., at pressure >1 bar, are not necessarily relevant to the Yucca Mountain repository which, it is anticipated, will remain vented after closure. Water vapor will displace air so the total pressure, ~1 bar, will determine the water vapor pressure.

The present study therefore has as its principal objective determination of the impact of heat on Portland cement and related compositions at temperatures in the range up to 200 °C at constant 1 bar water vapour pressure. Because the system is complex and the time factor is difficult to compress, certain simplifications had to be made. Thus, the experimental work used preformed $CaO–SiO_2–H_2O$ gels as starting materials and isobaric data obtained above 100 °C were confined to two isotherms: 130 and 200 °C. However, it was also possible to conduct experiments in the course of parallel programmes, which have resulted in a revised phase diagram for the $CaO–SiO_2–H_2O$ system at <200 °C and saturated steam pressure [2]. Additional solubility data for selected $CaO–SiO_2–H_2O$ phases at 25, 55 and 85 °C have also been obtained and are reported [3]. These data should be viewed in the broader context of understanding phase behaviour and solubilities in the $CaO–SiO_2–H_2O$ system across a broad range of compositions, temperatures and pressures.

2. Experimental

Homogeneous gels were prepared by the direct reaction method, by mixing carbonate-free $Ca(OH)_2$ with a chemically pure, high specific surface area amorphous silica: "Aerosil 300" (Degussa). Dry mixes were made at target Ca/Si molar ratios 2.0, 1.8, 1.6, 1.5, 1.4, 1.2, 1.0 and 0.85. The mechanical mixes were slurried into double-distilled, deionised and decarbonated water at an approximate water: solid weight ratio of 10. The resulting slurries were sealed into thick-walled polypropylene bottles equipped with closures known from previous experience to prevent CO_2 ingress. The contents were intermittently agitated with storage at 20±2 °C for 12–24 months. The bulk Ca/Si ratio of the solid portion was determined by chemical analysis using flame photometry for calcium and atomic absorption for Si. These analytically determined ratios are used in the tables and do not differ from target Ca/Si ratios by more than ±0.01–0.02. The gels were amorphous, or nearly so, to X-ray powder diffraction (XRD) except for Ca/Si ratio 2.01, which also contained $Ca(OH)_2$. Its content of $Ca(OH)_2$ was estimated at 8–10% by thermogravimetric analysis (TGA). Electron microscopy and diffraction also corroborated the presence of $Ca(OH)_2$ at ratio 2.01 in the form of tabular micron-sized, pseudo-hexagonal platelets.

To simulate the high Ca/Si ratio of C–S–H from "real" cements, often believed—without proof—to differ from "synthetic" C–S–H, Ca_3SiO_5 and Ca_2SiO_4 were prepared by repeated sintering of $CaCO_3–SiO_2$ mixes until phase pure, with subsequent hydration at 20±2 °C at a water:solid ratio of ~10. Following complete hydration, these preparations yielded mixtures of C–S–H and $Ca(OH)_2$.

Samples were sealed into PTFE bottles for ageing at constant temperatures at 25, 55 and 85 °C: only results from 55 and 85 °C are reported here. To avoid changes in the constitution of the silicate anions, gels were generally not dried. The moist gels were handled in CO_2-free N_2 atmosphere. Experiments at higher temperatures, 130 and 200 °C, were made in steam by modifying a conventional fan-assisted thermostated oven as shown in Fig. 1. Steam from a low pressure line was passed through a scrubber (not shown) and admitted into a heat exchanger to raise its temperature to that of the selected isotherm, either 130 or 200 °C, following which the steam was admitted into stainless steel canisters, each holding several cylinders of the same composition contained in open PTFE beakers. The cans and chamber were freely vented through an exit trap (not shown) to ensure that the overpressure did not exceed 2–5 Torr but also to ensure that air could not re-enter the chamber. The apparatus, although homemade, worked reliably and consistently. The accuracy of temperature control, ±2 °C, was monitored by a thermocouple. The nominal pressure, 1 bar, did, however, fluctuate with normal variations in barometric pressure characteristic of the local environment: the laboratory altitude is ~20 m above mean sea level.

Products were characterised by XRD, TGA and, where appropriate, by Fourier transform infrared spectroscopy and microscopy. Both scanning and transmission electron microscopy were used and the microscopes were equipped for chemical analysis; selected area electron diffraction was also undertaken in transmission mode. Bulk chemical analyses were made by atomic absorption (Si) and flame photometry (Ca). The ratios shown in the tables are those determined by actual analysis and are within experimental error, ±0.01, of the target composition expressed as molar Ca/Si ratio. Moreover, after exposure to flowing steam for up to 220 days, the initial Ca/Si ratio remained unchanged showing

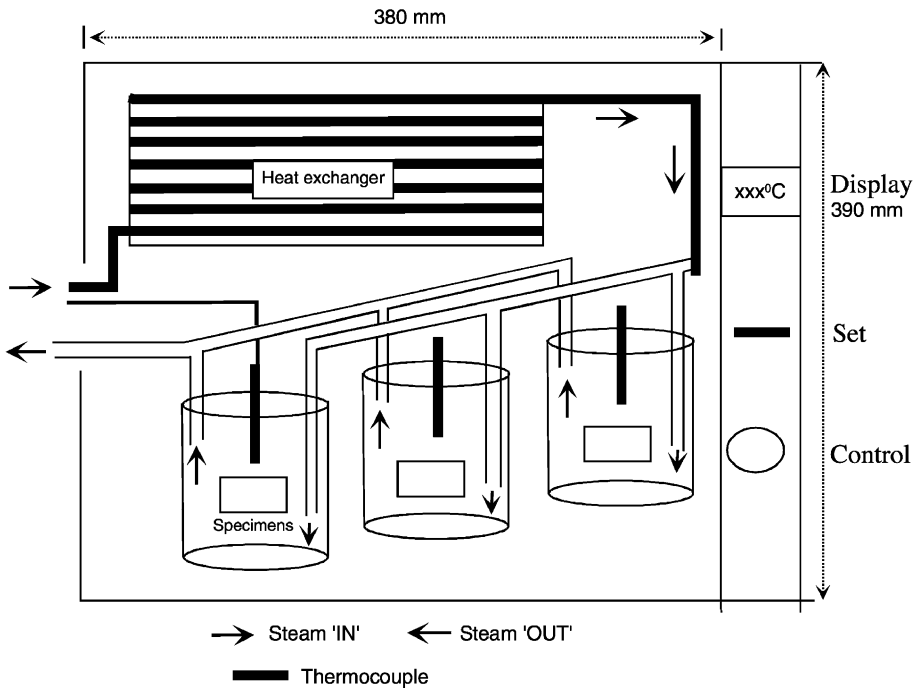

Fig. 1. Schematic representation of steam curing system in modified electric oven. Details of the quick release stop valve, which connects stainless steel specimen cans to steam entrance and exit lines, are omitted. The heat exchanger is a long length of copper tube soldered onto a finned copper plate. Arrows on the left show steam flow in (top) and out (bottom).

that neither $Ca(OH)_2$ or silica are volatile under the conditions of time and temperature used.

3. Results and discussion

3.1. Ageing in water: 25, 55 and 85 °C

Table 1 records the phase compositions of gels cured in liquid water at 25 and 55 °C for 730 days. Crystalline phases were identified mainly by XRD. C–S–H, unless present in large amounts and/or semicrystalline, may escape detection. Thus, all the samples treated at 55 °C are believed to contain residual C–S–H of low crystallinity. This is indirectly corroborated by weight loss curves obtained from D-dried product showing substantial water losses in the range 100–200 °C, which are characteristic of relatively amorphous C–S–H material. Nevertheless, the crystallinity of the C–S–H varies considerably. Particularly, at 25 °C, at which temperature much C–S–H persisted, the diffraction pattern of low Ca/Si ratio gels resembled that of the semicrystalline C–S–H (I) and on that account was readily detected by XRD. At 25 °C, C–S–H (I) was characteristic of low Ca/Si ratios, 0.83–1.20, whereas at higher ratios, 1.41 and more, a less C–S–H crystalline product was obtained.

Upon isothermal ageing, $Ca(OH)_2$ develops at Ca/Si ratios as low as 1.41 and, as the Ca/Si ratio of the preparation increased, increasing amounts of $Ca(OH)_2$ develop. The fresh precursor gels were however apparently free of $Ca(OH)_2$ up to and including ratio 1.80 and did not develop $Ca(OH)_2$ in the course of storage at 22 ± 3 °C. Portlandite development and the upper limit of homogenity of C–S–H are thus interdependent and change as a function of time and thermal history: see further discussion. At 25 °C, traces of 14 Å tobermorite nucleate at Ca/Si ratio 0.83 but were not observed to crystallise at other ratios. This tobermorite

Table 1
Development of crystalline phases in $CaO–SiO_2–H_2O$ compositions after 730 days at 25 and 55 °C

Molal Ca/Si	Initial state	Phases present at	
		25 °C	55 °C
0.83	C–S–H gel	C–S–H + [a]	14 Å Tob
1.01	C–S–H gel	C–S–H +	14 Å Tob
1.20	C–S–H gel	C–S–H +	11 Å Tob
1.41	C–S–H gel	C–S–H + Por (tr)	11 Å Tob
1.50	C–S–H gel	C–S–H + Por	Afw + 11 Å Tob + 14 Å Tob
1.60	C–S–H gel	C–S–H + Por	Afw + 11 Å Tob + 14 Å Tob
1.80	C–S–H gel	C–S–H + Por	Afw + Por + 11 Å Tob + 14 Å Tob
2.00	C–S–H gel + Por[a]	Por + C–S–H	Afw + Por + 11 Å Tob
3.00	C–S–H gel + Por[a]	Por + C–S–H	Por + Afw + 11 Å Tob

Por, $Ca(OH)_2$, (portlandite): Afw, afwillite; Tob, tobermorite, either (or both) 11 and 14 Å varieties; tr = trace.

[a] Made by hydration of Ca_2SiO_4 (Ca/Si = 2.0) and Ca_3SiO_5 (Ca/Si = 3.0).

appears to have precipitated from solution: well-developed sheet-like morphologies, sometimes forming clusters, were observed in transmission electron micrographs; corresponding selected area electron diffraction patterns gave tobermorite-like diffractions. It is considered that the relatively good morphological development of the tobermorite phase could only occur by nucleation and growth from the aqueous phase. The dissolution–precipitation process is facilitated by the congruent, or very nearly congruent, solubility of gels having the Ca/Si ratio ~ 0.83.

Crystallisation is more extensive at 55 °C than at 25 °C. Table 1 ranks the phases obtained in decreasing order of abundance, as judged from the relative strengths of their X-ray reflections. It is probable that C–S–H is present but its broad diffraction maxima cannot readily be deconvoluted in the presence of crystalline phases. The occurrence of afwillite among the products is not surprising; it is probably a thermodynamically stable phase at 55 °C. The form of tobermorite obtained at 55 °C is also a function of Ca/Si ratio: high Ca/Si ratios characteristically favour 11 Å tobermorite. The nature of the tobermorite obtained is thus sensitive to temperature and composition and the transformation between 11 and 14 Å, or vice versa, may not be a simple temperature-dependent transformation but instead reflects the Ca/Si stoichiometry of the reactants and possibly that of the solids: excess Ca in the bulk composition favours formation of the 11 Å phase.

3.2. Ageing in steam, 1 bar pressure, 130 and 200 °C

Table 2 shows the phases developed after treatment at >100 °C. Crystallisation is in general more complete at 130 °C than at 200 °C, although the composition at Ca/Si ratio 0.83 develops 11 Å tobermorite at both temperatures. Xonotlite develops at Ca/Si ratio 1.06, but only at 130 °C. Gel compositions having Ca/Si ratios greater than 1.5 exsolve $Ca(OH)_2$. Furthermore, X-ray reflections were obtained in one composition, Ca/Si = 1.81 treated at 130 °C, at 10.5° and 22° 2θ (CuKα radiation), which could not be assigned to any likely impurity, e.g., $CaCO_3$ or to any known calcium silicate hydrate except possibly calciochondrodite. However, calciochondrodite seems unlikely as its strongest reflections were absent.

Table 2
Development of crystalline phases in $CaO–SiO_2–H_2O$ compositions in steam, 1 bar pressure, at 130 and 200 °C

Molal Ca/Si	Phases detected by X-ray diffraction	
	130 °C, 120 days	200 °C, 90 days
0.83	11 Å Tobermorite	11 Å Tobermorite
1.01	Xonotlite	C–S–H
1.21	C–S–H (I)	C–S–H
1.50	C–S–H	C–S–H
1.81	C–S–H + $Ca(OH)_2$ + X[a]	C–S–H + $Ca(OH)_2$
2.01	C–S–H + $Ca(OH)_2$	C–S–H + $Ca(OH)_2$

[a] X refers to an incompletely characterised phase: see text.

Table 3
$Ca(OH)_2$ determinations (wt.%) by thermogravimetric analysis

Ca/Si ratio	24 months, 25 °C in liquid water[a]	130 °C, 120 days vapour, 1 bar	200 °C, 90 days vapour, 1 bar
0.85	0	0	0
1.01	0	0	0
1.21	0	0	0
1.50	0.9	0	0
1.81	5.3	3.0	1.5
2.01	11.8	6.0	5.1

[a] Results at 85 °C do not differ significantly from those at 25 °C.

3.3. $Ca(OH)_2$ and bound water determinations

The $Ca(OH)_2$ contents of the products were determined by thermogravimetry, with results shown in Table 3. The best quality data were obtained from 25 °C product; sloping backgrounds with complex curvature made determinations of $Ca(OH)_2$ in the higher temperature products, at 130 and 200 °C, less reliable. The values reported in Table 3 are believed likely to underestimate $Ca(OH)_2$ contents. Nevertheless, detectable free $Ca(OH)_2$ appears at Ca/Si ratios 1.81 and above. The amounts of free $Ca(OH)_2$ support the contention that the Ca/Si ratio of the remaining C–S–H phase decreases spontaneously in the course of heat treatment to ~ 1.5.

Table 4 shows the water contents of the gels after treatment at 130 or 200 °C. Experience of sampling at shorter treatment times showed that the water content had attained a steady state hence the results presented, especially

Table 4
Corrected water content of the $CaO–SiO_2–H_2O$ gel[a]

Ca/Si ratio	Temperature range, °C	Water content, wt.% of product after		
		25 °C/720 days in water	130 °C/120 days vapour, 1 bar	200 °C, 90 days vapour, 1 bar
0.83	25–105	7.2	3.2	1.8
	105–1000	10.3	8.2	8.1
	Total	17.5	11.4	9.9
1.01	25–105	7.0	2.1	1.1
	105–100	10.7	9.2	9.0
	Total	17.7	11.3	10.1
1.21	25–105	4.9	1.9	0.8
	105–1000	13.5	11.3	9.3
	Total	18.4	13.2	10.1
1.50	25–105	4.1	2.1	0.9
	125–1000	15.5	12.0	10.4
	Total	19.6	14.1	11.3
1.81	25–105	3.5	2.0	1.2
	105–1000	18.3	15.0	11.0
	Total	21.8	17.0	12.2
2.02	25–15	3.9	1.4	1.2
	105–1000	18.1	14.5	12.1
	Total	22.0	15.9	13.3

[a] After subtraction of water due to $Ca(OH)_2$; see Table 3.

for compositions whose content of crystalline phases is low, can be used as the basis for further calculation. These water contents are reported on material which had a preliminary and prolonged drying in flowing N_2 at 20 °C and are relative to ignited weight at 1000 °C; experience showed that the D-dried product gave virtually identical losses. The data are corrected for $Ca(OH)_2$ (portlandite) content as determined by TGA; other corrections are discussed as appropriate. However, the maximum correction for water held in $Ca(OH)_2$, applied to one high ratio Ca/Si (2.0) material, was ~10%.

The trends in bound water compositions are shown in Fig. 2. At 25 °C the total water contents of gels increase slightly as the Ca/Si ratio increases. However, the balance of water loss shifts: the proportion lost at <105 °C decreases slightly as the Ca/Si ratio increases, while the proportion of more strongly bonded water lost at >105 °C increases with increasing Ca/Si ratio. In every case, the absolute water loss at fixed Ca/Si ratio decreases with increasing temperature.

Comparison of data on water contents also needs to take into account the extent to which crystallisation has occurred. As noted, experimental uncertainties make it impossible to measure residual gel contents except indirectly. For example, at Ca/Si ratio 0.83, tobermorite crystallises at both 130 and 200 °C. If we assume the composition of 11 Å tobermorite is $C_5S_6H_5$, the theoretical loss based on the ignited weight would be 90/640.6, or 14%. Relative to this benchmark the 130 °C product is only slightly deficient in water, although the 200 °C product is markedly deficient and cannot therefore consist of phase pure 11 Å tobermorite. The composition at Ca/Si = 1.01 yielded xonotlite at 130 °C and had 9.2% loss at >105 °C. Had it completely converted to xonotlite, no significant loss should have occurred at <105 °C while the loss at >105 °C would have been 2.6%, assuming the C_6S_6H formula. A TGA of this sample, using the size of the characteristically steep loss step, gave an estimated phase purity of 40% xonotlite. While substantial error, perhaps ± 10%, attaches to this measurement it is concluded from two independent methods that conversion to xonotlite is incomplete. This distinction, between pure phases and phase mixtures, becomes important in assessing solubilities and pH-conditioning of the solids upon a coexisting aqueous phase.

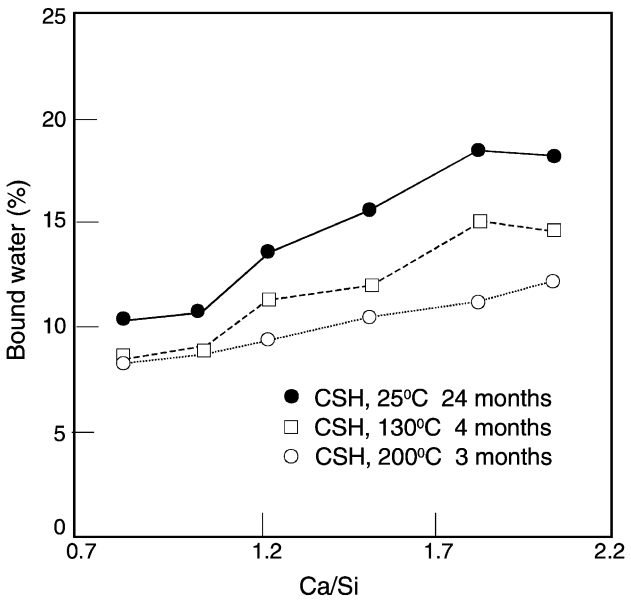

Fig. 2. Bound water contents of C–S–H gels. The numerical values have been corrected for $Ca(OH)_2$ impurity and in one case for xonotlite content.

Comparing treatments at 130 and 200 °C, and restricting comparison to largely noncrystalline preparations, the content of water is reduced by high temperature treatment. Very little of the remaining water in 200 °C product can be removed upon subsequent drying at <105 °C. The amount of water retained to higher temperature, >105 °C, is therefore substantial and is in theory sufficient to form all but the more highly hydrated crystalline phases of the $CaO–SiO_2–H_2O$ system. The virtual absence of crystallisation in most compositions at 200 °C is therefore attributed to kinetic factors rather than to a chemical shortage of retained water, resulting from dehydroxylation.

3.4. Composition and nanostructure of C–S–H

Electron diffraction studies of the C–S–H gels made in the course of the present study confirm the lack of long-range order among gels aged 1–2 years at 25 °C. Their diffraction patterns give mainly smooth broad powder arcs. However, upon ageing at 55 °C and above, the gels develop structure. This structure is evident from the appearance of sharp diffraction maxima in selected area diffraction patterns, often superimposed on powder arcs and suggesting a diphasic structure. High resolution transmission electron micrographs confirm this: small, ca. 500–1000 nm C–S–H foils, reveal a complex internal mosaic of nanoscaled domains shown in Fig. 3. The image shows numerous zones of two types: one consists of nanoscale regions of $Ca(OH)_2$ and the other of nanocrystalline C–S–H domains. The appearance of both types is sensitive to orientation and not all features show in any single image. The C–S–H domains are strikingly similar to those reported by Viehland, except for the additional presence of $Ca(OH)_2$ [4]. The multiplicity of reflections obtained from composites precludes assigning the C–S–H domain structures to a particular crystalline phase (e.g., to tobermorite or jennite) although the patterns obtained would not be inconsistent with either assignment. The resulting nanostructures formed are very similar to those formed in certain organic high polymer systems in which "crystalline" regions are dispersed in an "amorphous" matrix [5]. The analogy with organic polymers helps explain the origins of nanostructures of compositions in the Ca/Si range between 0.85 and 1.4 approximately. However, at ratios 1.5 and above, this nanostructure is additionally complicated by the appearance of $Ca(OH)_2$ crystallites. These crystallites, typically only a few

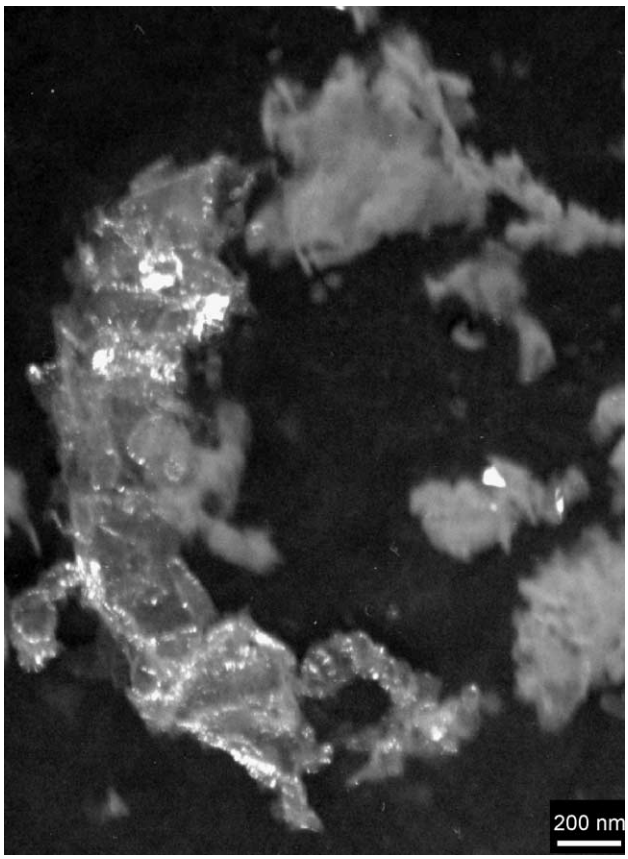

Fig. 3. Transmission electron micrograph of C–S–H, Ca/Si = 1.7, treated in steam, 1 bar pressure, at 130 °C for days. The bright field images supplemented by electron diffraction show nanoscale crystallisation of C–S–H as well as segregation by exosolution of $Ca(OH)_2$. Domain sizes are typically on the order of 100 nm or less.

tens of nanometers in size, decorate the textured C–S–H and give a set of electron diffractions which are unambiguously attributable to portlandite. Moreover, at Ca/Si ratios above 1.5, the density of portlandite precipitation increases as the Ca/Si bulk ratio increases. Thus at or above Ca/Si ratio 1.5 two processes occur in the stream-treated compositions; exsolution of $Ca(OH)_2$, with decrease in the Ca/Si ratio of the remaining C–S–H and nanoscale crystallisation within C–S–H. These features are only apparent by electron microscopy and diffraction and are not detected by conventional XRD.

Direct evidence for reduction of Ca/Si ratio of the C–S–H portion as a consequence of portlandite nucleation was sought by transmission electron microscopy with analysis. It is of course difficult to find regions free from portlandite and, as the Ca/Si ratio increases, it becomes progressively more difficult to isolate regions apparently consisting only of C–S–H. The results of analyses are shown in Table 5. The best results, having the lowest standard deviations, are obtained for Ca/Si = 0.85: this preparation is believed to remain compositionally homogeneous and its mean Ca/Si ratios lie well within one standard deviation of the bulk ratio, as determined by bulk chemistry. At bulk Ca/Si = 1.50 and 1.81, standard deviations increase. However, the analytical Ca/Si ratio at target bulk Ca/Si ratio 1.5 is about one standard deviation less than the chemically determined ratio and this increases to approximately two standard deviations at bulk ratio 1.81. Our interpretation of these data, coupled with the confirmed appearance of $Ca(OH)_2$, is that the limit of homogeneity of C–S–H in heat-treated samples is essentially independent of bulk composition and lies between Ca/Si = 1.45 and 1.50. Higher ratios can be made which are homogeneous at ~25 °C, but these are labile and, if cured in steam at 1 bar, readily exsolve $Ca(OH)_2$, initially in the form of nanoscale crystallites which do not record in XRD patterns. This $Ca(OH)_2$ is not, however, "amorphous" as it gives sharp electron diffraction patterns. In the absence of liquid water, nanoscale $Ca(OH)_2$ crystals are unable to dissolve and reprecipitate as larger crystals and therefore persist. Upon heating in air, these nanoscale crystallites lose water over a broad range of temperatures and are not readily detected by thermogravimetry, which depends on a relatively sharp step occurring at ~450 °C. Thus, the apparent content of $Ca(OH)_2$ (Table 3) tends to be lower than the true content with differences increasing as the bulk Ca/Si ratio increases in the range above ~1.5.

3.5. Solubility properties of C–S–H

One of the most important properties of cements in the present context is their ability to condition the pH of permeating water. Therefore, the pH conditioning ability of thermally treated preparations were measured by placing ~1 g in ~20 ml of initially deionised, double-distilled water. The pH and Ca solubilities were measured after ~7 days of gentle agitation. The results are depicted in Fig. 4. Solid diamonds represent points determined by Atkinson et al. [6], which are, in turn, very similar to others reported in the literature. The literature data disclose two regions of pH conditioning at higher Ca/Si ratios (>0.8, approximately). At Ca/Si>1.5–1.8, C–S–H begins to coexist with portlandite such that the coexistence of the two phases defines a univariant equilibrium: at constant pressure, solubility and pH are defined by temperature so on an isothermal plot the two solids condition constant pH in solution. Of course, the same situation obtains at Ca/Si ratios >1.8. At lower Ca/Si ratios, such that one phase—C–S–H of variable composition—occurs, the aqueous pH is not fixed and it is necessary to define the Ca/Si ratio in order to ensure a constant

Table 5
Ca/Si ratio of C–S–H in heat-treated preparations

Bulk Ca/Si ratio	Ca/Si ratio of C–S–H with (S.D.)	
	C–S–H vapour, 130 °C, 90 days	C–S–H vapour, 200 °C, 60 days
0.85	0.83 (0.05)	0.83 (0.07)
1.50	1.40 (0.09)	1.39 (0.08)
1.81	1.62 (0.12)	1.65 (0.07)

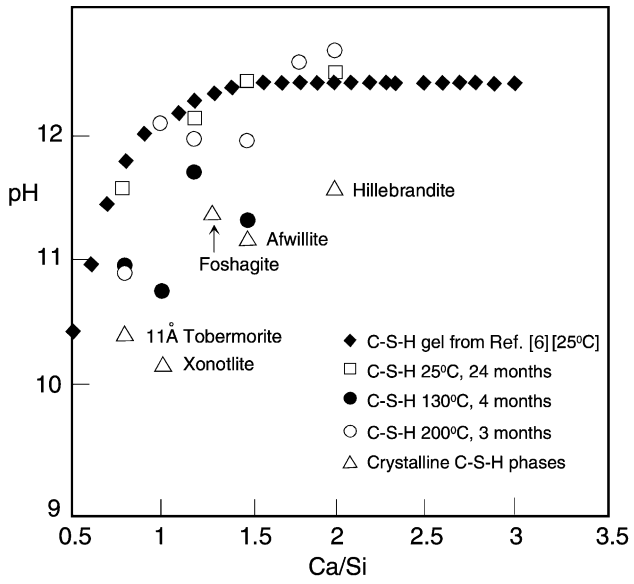

Fig. 4. The pH of solutions equilibrated with C–S–H solids either fresh (diamonds/open squares), after heat treatment at 130 °C (closed circles) or 200 °C (open circles). These are compared with the self-generated pH of synthetic crystalline calcium silicates (triangles). See text for discussion.

equilibrium pH of a coexisting solution on an isotherm. Data for selected C–S–H crystalline phases believed to be stable at ~25 °C are also shown Fig. 4. These lie well below the solubility of the metastable assemblages with C–S–H, if comparison is restricted to the same Ca/Si ratio. Data for the crystalline phases are taken from Hong [3]; another set of solubility data currently in preparation are not expected significantly to alter these numerical values [7]. Open squares show data obtained in the course of the title study from C–S–H prepared and aged at 25 °C. These do not differ significantly from many others reported in the literature. Data obtained from gels cured in steam, 1 bar, at 130 °C are shown by closed circles. At high Ca/Si ratios, 1.7 and 2.0, the data points lie within limits of error at the same pH obtained from fresh gels at the same rates. This is not surprising since the 130 °C treatment results in exsolution of $Ca(OH)_2$, so the pH becomes effectively conditioned by the solubility of $Ca(OH)_2$ and its coexistence with C–S–H. At lower Ca/Si ratios, such that exsolved $Ca(OH)_2$ is absent, the pH conditioning ability of steam-cured gels lies somewhat below the trend line for fresh, nearly amorphous gels. This is attributed mainly to internal nanoscale crystallisation, which lowers the relative free energy compared to amorphous product: the extent of pH reduction is on the order of 0.5–1.0 pH unit.

4. Additional discussion

In comparing results obtained in the course of the present studies with those obtained previously, a distinction should be made between experiments made at <100 °C and those at >100 °C. Experiments at >100 °C were made in steam, whereas those described in the previous literature were made in water. We can find only one exception: Imlach and Taylor [8] cured in saturated steam, at 140 and 170 °C, and subsequently treated products at the same temperature, in superheated steam. Their results are broadly comparable with those in Table 2. Decreasing the activity of water, in this instance by reducing steam pressure on any isotherm above 100 °C from saturation pressures to 1 bar, has a dehydrating effect on the phases formed.

It is apparent that ageing of C–S–H, especially at above ambient temperatures, has a substantial impact on the constitution of this phase. Because fresh gel is nearly amorphous and ranges in composition, many classical methods used to characterise its phase properties are inapplicable, or applicable only with modification. The following discussion concerns alumina-free C–S–H. We do not as yet know if the data presented here apply to "real" C–S–H—the phase occurring in Portland cement but also containing minor alumina and sulfate—but it is expected that the same phenomena will occur. In support of this, C–S–H product obtained from hydration of chemically pure Ca_3SiO_5 and Ca_2SiO_4 gives numerical data, which, within experimental error, agree with those obtained from appropriate synthetic gels. The C–S–H product is of course diphasic and contains much $Ca(OH)_2$ as well as C–S–H.

Figs. 5 and 6 correlate data obtained in the course of the present study with those in the literature. Fig. 5 shows schematically the evolution of structure and composition at low temperatures, <130 °C but mainly at <85 °C. Commencing with nearly amorphous material, the pathways diverge according to Ca/Si ratio; all "gels" improve in crystallinity upon ageing, but additionally those with Ca/Si ratios in excess of 1.5, approximately, will exsolve $Ca(OH)_2$. The time required for these processes to occur is not known with accuracy: qualitatively, it diminishes with increasing temperature. In the absence of liquid water, which allows dissolution and reprecipitation processes to occur the final

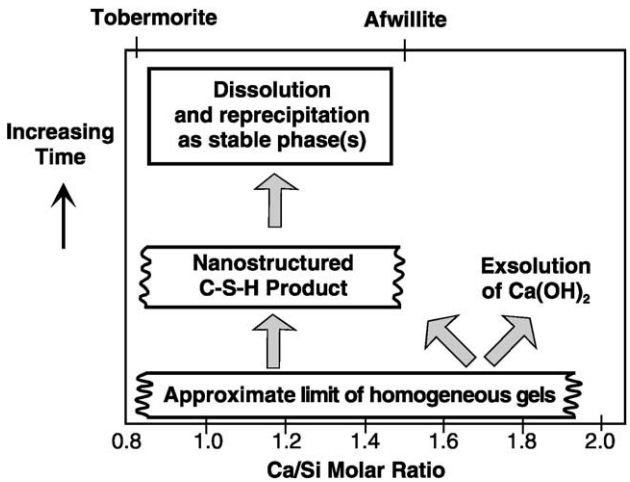

Fig. 5. Evolution of structure/composition in steam cured C–S–H gels.

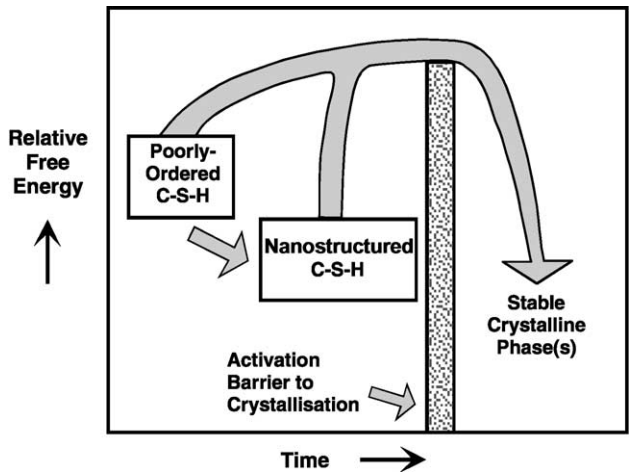

Fig. 6. Energetics of C–S–H and its crystalline products.

stages of reaction, which require formation of crystalline phases with microscopic phase boundaries, must occur slowly at 130 °C.

Fig. 6 depicts schematically the energetics of the process in vapour. The activation barrier to crystallisation in the usual sense undoubtedly comprises several factors, but given the wide range of crystalline $CaO–SiO_2–H_2O$ phases stable at 130–200 °C, no composition having $Ca/Si \leq 1.5$ lies far from that of a stable crystalline phase, so we suppose that the activation barrier arising from the need to diffuse chemical constituents remains approximately constant. If, however, the initially labile gel can lower its free energy, it is more difficult subsequently to overcome the activation barrier, with the result that crystallisation is impeded. This reduction in free energy is reflected in the diminished solubility, relative to a less-structured gel of the same composition, achieved following development of an internal nanostructure. Presumably, this in part explains received wisdom in the autoclaved cement industry namely, that in a fixed autoclaving time, typically a few hours, yields of crystalline phases are improved by using fresh gel products: well-cured gels formed at or near ambient temperatures do not crystallise readily upon application of high temperatures.

The introduction outlined the characteristics of a nuclear waste repository at 1 bar pressure subject to a prolonged thermal excursion. In order to predict the future behaviour of cement in such conditions, we have to define the boundaries of the reactive system: does it include only cement or does it also include mineral aggregates used in concrete as well as those which comprise the country rock? And if so, to what extent: where are the system boundaries? These questions are difficult to answer in general but if we narrowly define the system as consisting of cement only, it will have an initial Ca/Si ratio in the range 2.5–3.0, i.e., typical for a modern Portland cement. Upon hydration it will contain $\sim$20% $Ca(OH)_2$, which buffers pH. This $Ca(OH)_2$ will persist throughout the thermal cycle and, moreover, will be added to as additional $Ca(OH)_2$ exsolves from C–S–H, the Ca/Si ratio of which decreases. This is an irreversible process, the direction of which will not be reversed during the subsequent decay of the thermal pulse and return to ambient temperatures. So in this defined system and in the absence of leaching, a quantitatively large reserve of $Ca(OH)_2$ will remain to buffer pH to >12 at 25 °C. However, we must also consider the subsequent evolution of the system, as well as possible reactions with the local environment.

As long as concrete temperatures remain at or slightly above 100 °C, relatively little will occur to diminish the $Ca(OH)_2$ content. However, once water returns and permeates the concrete, $Ca(OH)_2$ will be reduced by leaching as well as by reaction with groundwater components such as bicarbonate, resulting in conversion of portlandite to calcium carbonate. Considering only the contribution of leaching, large volumes of pure water would have to percolate concrete before pH diminishes to that of the background. Indeed, if rapid diminution of pH is to be achieved, it would be necessary to look to a broader definition of the system, for example by assessing the potential for cement–aggregate interactions to reduce pH. A siliceous aggregate might well react in two stages, consuming much or all free $Ca(OH)_2$ in the first stage, and lowering the Ca/Si ratio of C–S–H in the second with the added prospect of crystallisation of C–S–H. The cumulative impacts would greatly reduce pH in the post-thermal pulse stage. Thus proportioning of concrete, which typically contains as little as 12–24 wt.% cement, is such that, in conjunction with a siliceous aggregate and a prolonged thermal pulse, the post-thermal pulse pH may significantly and permanently decrease. Lacking quantitative inputs, it is difficult to calculate the extent of reduction, but pH values in the range 9–10 should be attainable assuming typical concrete mix properties. In conclusion, therefore, it is unlikely that the pH conditioning ability of Portland cement would be affected by a transient thermal pulse lasting perhaps several decades. However, reaction with groundwater, especially carbonate containing water, as well as with siliceous aggregates normally used in concrete have potential to significantly and permanently to reduce pH in the post-thermal pulse stage.

Acknowledgements

The financial support of the Southwest Research Institute, Project No. 20-/402, is gratefully acknowledged.

References

[1] H.F.W. Taylor, Cement Chemistry, Academic Press, London, 1990.
[2] S.-Y. Hong, F.P. Glasser, Phase relations in the $CaO–SiO_2–H_2O$ system, 25°–200 °C, at saturated steam pressure, Adv. Cem. Res. (submitted).
[3] S.Y. Hong, Calcium silicate hydrates: crystallisation and alkali sorption, PhD Thesis, University of Aberdeen, 2000.

[4] D. Viehland, J.F. Li, L.H. Yuan, Z. Xu, Mesostructure of calcium silicate hydrate (C–S–H) gels in Portland cement paste: short range ordering, nanocrystallinity and local compositional ordering, J. Am. Ceram. Soc. 79 (1996) 1731–1744.
[5] A.R. Jenkins (Ed.), Polymer Science—A Materials Science Handbook, vol. 1, North Holland, Amsterdam, 1972, pp. 251–276 (Chapter 4).
[6] A. Atkinson, J.A. Hearne, C.F. Knights, Aqueous chemistry and thermodynamic modelling of $CaO–SiO_2–H_2O$ gels, J. Chem. Soc., Dalton Trans. (1989) 2371–2379.
[7] C.L. Dickson, D.R.M. Brew, F.P. Glasser, Solubilities of $CaO–SiO_2–H_2O$ phases at 25°, 55° and 85 °C, Cem. Concr. Res. (submitted).
[8] B.F. Imlach, H.F.W. Taylor, Prolonged hydrothermal treatment of cement mixes: Part III. Autoclave curing of C_3S–calcite pastes, Trans., J. Br. Ceram. Soc. 71 (1972) 81–83.